Passivity-Constrained Digital Twins for Dissolution-Buffered Gas Kicks in Managed Pressure Drilling

Chamod Fernando[1] and Ravindu Senanayake[2]

[1]Sabaragamuwa University of Sri Lanka, Belihuloya 70140, Sri Lanka
[2]Rajarata University of Sri Lanka, Mihintale 50300, Sri Lanka

Abstract

Drilling in narrow pressure windows increasingly depends on managed pressure drilling, where choke and pump actuation continuously reshape annular boundary conditions. These operational advantages complicate early kick interpretation because surface measurements reflect both physical disturbances and deliberate control transients. In oil-based and synthetic-based systems, additional ambiguity arises when invading gas dissolves into the liquid phase and induces swelling, changing volumetric returns and effective density without an immediately dominant free-gas holdup. This paper develops a passivity-constrained digital-twin architecture for real-time diagnosis and safety monitoring of dissolution-buffered gas kicks. The technical contribution is an energy-based state-space formulation of annular hydraulics with explicit dissolved-gas inventory and swelling-modified constitutive relations, cast into a port-Hamiltonian structure with provable dissipation under friction and bounded thermodynamic exchange. This structure is leveraged to construct structure-preserving discretizations and passivity-based observers whose error dynamics admit incremental energy bounds even under time-varying boundary actuation and sensor bias. A certificate layer maps the digital-twin energy balance into conservative online bounds on bottomhole-pressure deviation and on surface gas-handling risk proxies over short horizons, enabling decision thresholds that remain valid under closure uncertainty. Numerical studies show that passivity constraints stabilize estimation during aggressive choke maneuvers, prevent unphysical state excursions near phase appearance, and improve discrimination between swelling-driven pit gain and free-gas expansion when measurements are sparse. The resulting framework provides a tractable pathway to integrate dissolution physics into safety-critical monitoring without requiring full multiphase simulators in the real-time loop.

1 Introduction

Managed pressure drilling has shifted the operational baseline for wells with small margins between pore pressure and fracture pressure [1]. By actively manipulating surface backpressure and circulation conditions, operators can shape the bottomhole pressure trajectory rather than accept it as a passive outcome of hydraulics. The same actuation authority that improves controllability, however, complicates diagnosis. When choke setpoints, pump rates, and surface equipment dynamics continuously vary, the mapping from downhole states to surface measurements becomes time dependent and often non-intuitive. Pressure fluctuations that appear anomalous in a static setting may be routine under active control, while early-stage influx signals can be partially masked by deliberate boundary changes. A digital twin used in this context must therefore handle strong input forcing and partial observability, and it must do so without producing fragile inferences that depend on narrow modeling assumptions.

A second complication arises from thermodynamic partitioning of invading gas in oil-based and synthetic-based fluids [2]. Dissolution can delay the appearance of a distinct free-gas phase and can produce liquid swelling that modifies volumetric return and density. This leads to a non-uniqueness in early indicators such as pit gain: similar pit-volume trajectories can correspond to very different internal inventories of free and dissolved gas, and these inventories imply different near-term hazards. In particular, a swelling-dominated regime can raise pit-capacity and density-related concerns without immediate surface gas-handling limits, whereas a free-gas-dominated regime can quickly drive surface gas rates and compressibility-driven pressure transients. Thermodynamic modeling has established that this buffering is not merely qualitative. Manikonda et al. (2020) provided a pioneering thermodynamic framework that quantified kick-gas dissolution into oil-based drilling fluids and linked solubility

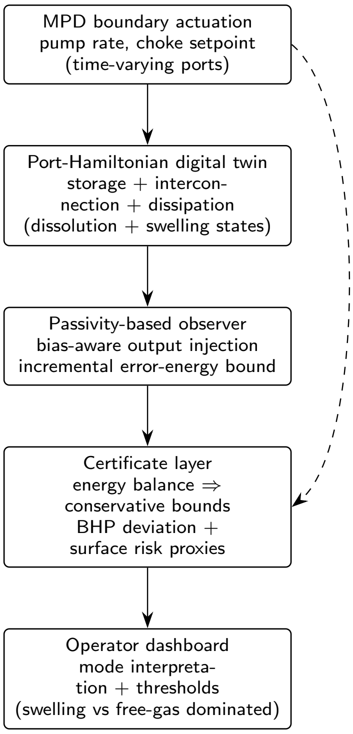

Figure 1: Passivity-constrained digital-twin stack for managed pressure drilling under dissolution buffering. Boundary actuation enters through power-consistent ports, a port-Hamiltonian core enforces dissipation and bounded exchange, passivity-based observers provide stable estimation under aggressive forcing and sensor bias, and an energy-certificate layer maps stored energy and dissipation into conservative online bounds for bottomhole-pressure deviation and short-horizon surface-handling risk proxies.

behavior to operationally relevant volumetric effects [3], motivating the inclusion of dissolved inventory and swelling response as explicit states rather than as ad hoc corrections.

Digital-twin development for drilling has often emphasized either high-fidelity simulation or data-driven pattern recognition. High-fidelity multiphase simulators can capture distributed transport and phase behavior but are frequently too costly or too brittle for continuous assimilation, especially when closure uncertainty is large and when repeated forward solves are required for estimation [4]. Data-driven detectors can be fast, but they can struggle with regime shifts and can be difficult to certify for safety-critical decisions, particularly when the underlying physics couples signals in nonlinear ways under actuation. The present work targets a different requirement: the digital twin should be structurally compatible with safety certification and should remain stable under aggressive boundary forcing and uncertain closures. This requirement suggests a modeling approach that encodes invariants and dissipation properties explicitly, so that estimation and prediction do not rely solely on numerical tuning or on short-window correlations.

Energy-based modeling provides a natural route. Annular hydraulics is a dissipative dynamical system in which compressibility stores energy, gravity stores potential energy, friction dissipates energy, and boundary actuation injects or extracts power. When dissolution and swelling are relevant, additional internal storage and exchange appear: dissolved gas represents an inventory whose equilibrium depends on pressure and temperature, and swelling modifies density and volume relations that govern hydrostatics and surface returns [5]. If these mechanisms are encoded within a passivity or port-Hamiltonian structure, then stability properties can be preserved under discretization and exploited in observer design. Passivity is particularly attractive because it yields input-to-state bounds and incremental energy inequalities that remain meaningful under time-varying inputs, which is precisely the managed pressure setting.

The thesis of this paper is that passivity-constrained digital twins provide a practical foundation for dissolution-aware monitoring because they couple three desirable properties in a single architecture. First, the port-Hamiltonian structure enforces physically consistent energy exchange at boundaries, preventing the digital twin from generating spurious energy under actuation and reducing the likelihood of unphysical state excursions. Second, passivity-based observers can be constructed so that estimation error obeys a dissipative inequality, yielding robust convergence behavior even when measurements are sparse and biased. Third, the same energy inequality can be mapped into conservative certificates on safety-relevant outputs, enabling decision thresholds that are not merely heuristic but are grounded in a bound on system energy and dissipation.

The technical contribution is not to propose a new empirical correlation for solubility or friction, nor to construct

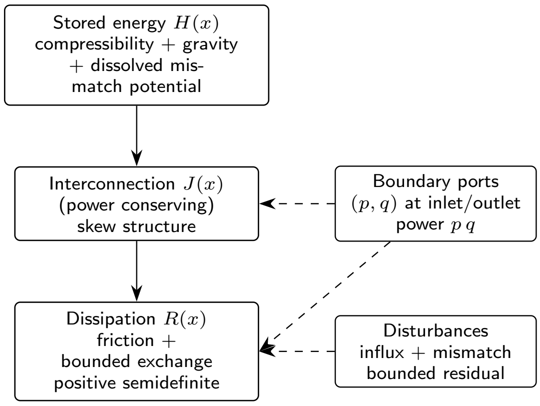

Figure 2: Port-Hamiltonian decomposition of a dissolution-aware annular twin. Energy storage captures compressibility, hydrostatics, and an internal convex potential that penalizes mismatch between dissolved inventory and equilibrium; skew interconnection conserves power; dissipation aggregates friction and bounded thermodynamic exchange; boundary ports expose power-consistent actuation and measurement interfaces for MPD.

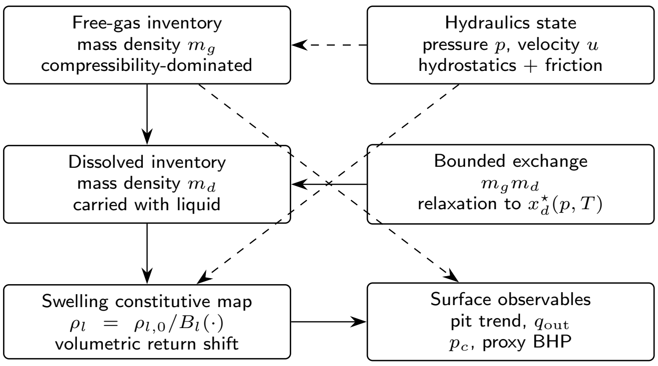

Figure 3: Dissolution-buffered state partitioning inside a passivity-constrained twin. Free and dissolved inventories evolve with a bounded exchange operator driven by equilibrium maps, while swelling modifies constitutive relations that govern density and volumetric returns. This explicit partition supports stable interpretation of pit trends that may not correspond to immediately dominant free-gas holdup.

a high-fidelity multiphase simulator [6]. The contribution is a structured formulation and estimation method that accommodates dissolution and swelling as uncertain but bounded mechanisms and that produces conservative, real-time safety indicators. The approach is intended to complement existing control systems rather than replace them. It can operate alongside managed pressure controllers, using the same input signals and surface measurements, providing a real-time estimate of hidden inventories and a certificate of whether a particular deviation is consistent with safe operation under the current uncertainty representation.

The remainder of the paper develops this architecture. A modeling section introduces an annular hydraulics state representation that includes free and dissolved gas inventories and swelling-modified constitutive relations, and it defines boundary ports consistent with managed pressure actuation. A structural section casts the model into a port-Hamiltonian form and derives an energy balance with explicit dissipation and exchange terms, including a bounded representation of thermodynamic dissolution. A discretization section constructs a structure-preserving semi-discrete model and discusses how positivity and boundedness are maintained without non-physical projection that would break passivity [7]. An estimation section derives passivity-based observers and parameter adaptation laws, including handling of sensor bias and closure uncertainty, and it introduces incremental energy bounds for estimation error. A certification and evaluation section maps energy bounds into conservative indicators for bottomhole-pressure deviation and surface risk proxies, and it reports numerical studies illustrating stability and interpretability in swelling-buffered and free-gas-dominated regimes. The paper concludes by summarizing implications and limitations.

2 Dissolution-Aware Annular State Representation and Boundary Ports

A passivity-constrained digital twin must be expressed in variables that admit a meaningful storage function and power-conjugate boundary ports. The annulus is treated as a one-dimensional conduit along measured depth, with coordinate $z \in [0, L]$ from the bit at $z = 0$ to the surface outlet at $z = L$. The state representation is selected to

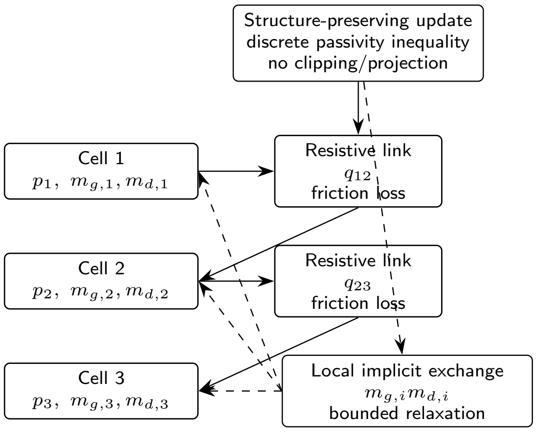

Figure 4: Structure-preserving semi-discrete realization for real-time deployment. A low-order chain of pressure-storage cells interconnected by resistive flow links maintains a discrete passivity inequality, while dissolution exchange is handled via local implicit bounded updates that conserve total gas mass per cell without non-physical state projection.

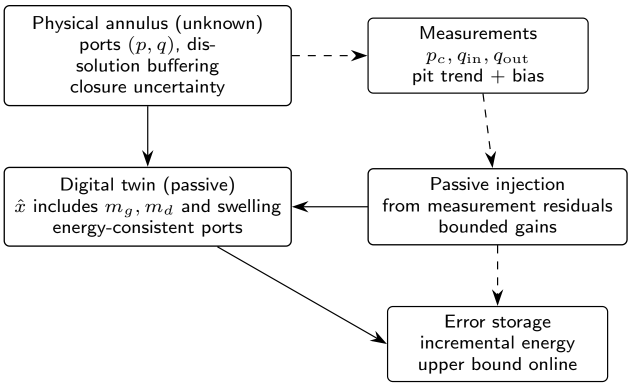

Figure 5: Passivity-based observer structure for stable estimation under aggressive MPD forcing. Measurement residuals enter through a passive injection channel with bounded gains, yielding an incremental error-energy storage that remains bounded under sensor bias and closure mismatch, while preventing unphysical excursions of free/dissolved inventories near phase appearance.

retain the dominant coupling among pressure, volumetric returns, and gas partitioning while remaining compatible with low-order discretization and real-time computation [8].

The model tracks a compressible mixture whose mass and momentum dynamics are influenced by a free-gas phase and a swollen liquid phase. The gas inventory is partitioned into a free component and a dissolved component. The dissolved component is not modeled as a separate moving phase; instead, it is modeled as a scalar inventory carried with the liquid that modifies liquid specific volume through swelling. This choice reflects the operational fact that dissolution can materially influence pit-volume and density without requiring immediate free-gas holdup, and it provides a mechanism by which pressure modulation can shift the partition between free and dissolved inventories. The model therefore introduces a dissolved gas mass fraction $x_d(z,t)$ in the liquid, a free-gas volume fraction $\alpha_g(z,t)$, and pressure $p(z,t)$ and mixture velocity $u(z,t)$ as primary hydraulic variables.

To preserve conservation and to support energy analysis, it is useful to express the gas inventory in mass form rather than in volumetric form. Let $m_g(z,t)$ denote free-gas mass density and $m_d(z,t)$ denote dissolved-gas mass density, both per unit mixture volume [9]. These quantities satisfy transport balances with exchange. The exchange term is driven by an equilibrium dissolved fraction $x_d^\star(p,T)$ and by a kinetic rate parameter κ_d, but within the digital-twin architecture these are treated as uncertain within bounds rather than as fixed scalar values. This choice is motivated by limited compositional information and by uncertainty in temperature profiles.

The swollen liquid density ρ_l is modeled as a base density divided by a swelling factor B_l. The swelling factor is a bounded, smooth function of dissolved fraction and state. Gas density ρ_g is modeled as a compressible function of pressure and temperature, typically via a compressibility factor. The mixture density ρ_m is then derived from free and liquid contributions, and the mixture momentum equation is written in terms of mixture velocity and pressure [10]. This mixture-level momentum balance is not intended to resolve detailed two-fluid dynamics. Its purpose is to capture the energetics of pressure work, kinetic energy, gravity, and friction in a form that admits a dissipation inequality.

In a managed pressure setting, boundary conditions are not fixed values but are ports through which power flows.

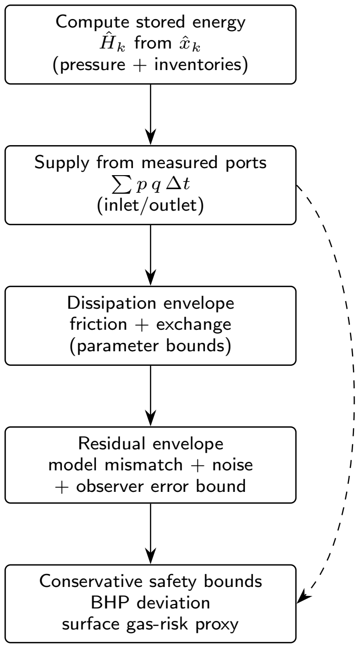

Figure 6: Energy-balance certification pipeline. The twin computes stored energy from estimated states and aggregates measured boundary power over a short horizon; dissipation and mismatch are bounded using closure envelopes and observer error-energy bounds; the resulting inequality yields conservative online bounds on bottomhole-pressure deviation and short-horizon surface risk proxies even when dissolution buffering and swelling alter pit and density signatures.

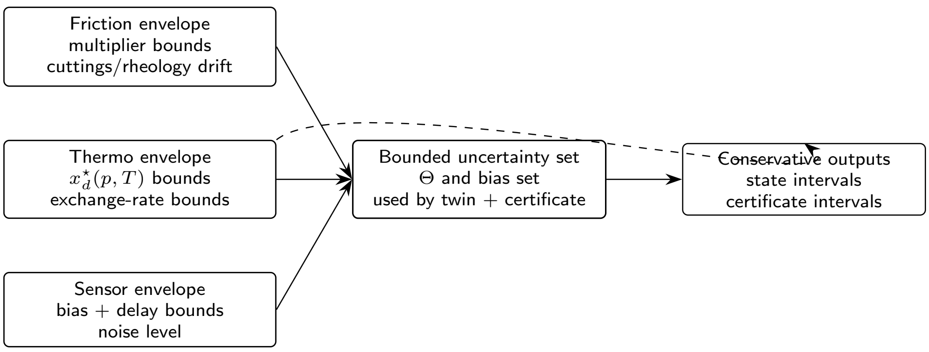

Figure 7: Uncertainty representation designed for passivity and certification. Rather than relying on precise closures, the twin operates over bounded envelopes for friction, thermodynamic equilibrium/exchange, and sensor imperfections. These envelopes enter both the observer (to prevent drift) and the certificate (to produce conservative safety bounds) while remaining compatible with real-time computation.

At the surface, the choke imposes a relation between outlet pressure and outflow, and casing pressure setpoints can inject or remove energy. At the inlet, the pump imposes an inflow rate and standpipe pressure dynamics that inject power. These boundary interactions are naturally expressed in terms of pressure and volumetric flow, which are power conjugate in hydraulics [11]. The port variables are therefore taken as boundary pressure $p_b(t)$ and boundary volumetric flow $q_b(t)$ at each boundary, with instantaneous power $P_b(t) = p_b(t)\, q_b(t)$, with sign conventions chosen consistently.

The surface measurements available to the digital twin are typically $p_c(t)$, $p_{sp}(t)$, $q_{in}(t)$, $q_{out}(t)$, and pit-volume change. These measurements do not provide direct access to internal states such as m_d or α_g. The digital twin must infer these from the way they influence observable ports and volumetric balances. Swelling affects the mapping from mass flow to volumetric flow, and dissolution affects the timing and magnitude of free-gas release. Both affect the pressure field through density and compressibility. The state representation is thus designed so that dissolution and swelling influence the same observables that drive operational decisions, while still being amenable to energy-based analysis.

Uncertainty enters through closure parameters and through latent initial conditions [12]. Gas property correlations affect density and viscosity and thus friction and hydrostatics. Property-correlation error can be several percent in relevant regimes [13], which is small in steady calculations but significant in transient inference near constraint bounds. Friction coefficients vary with cuttings loading and rheology, and the dissolution kinetic rate

Variable	Symbol	Description	Role in digital twin
Pressure field	$p(z,t)$	Mixture pressure along the annulus	Primary driver of hydrostatics and compressibility storage
Mixture velocity	$u(z,t)$	Cross-sectional average axial velocity	Governs convective transport and frictional dissipation
Free-gas volume fraction	$\alpha_g(z,t)$	Local fraction of free gas in the mixture	Controls compressible storage and free-gas expansion signatures
Dissolved-gas mass fraction	$x_d(z,t)$	Gas mass fraction carried in the liquid	Encodes dissolution buffering and swelling response
Free-gas mass density	$m_g(z,t)$	Free-gas mass per unit mixture volume	Links gas inventory to surface gas-handling proxies
Dissolved-gas mass density	$m_d(z,t)$	Dissolved-gas mass per unit mixture volume	Captures hidden inventory that may exsolve under depressurization
Mixture density	$\rho_m(z,t)$	Combined liquid and gas density	Affects gravitational storage and ECD-related constraints

Table 1: Dissolution-aware hydraulic state variables retained in the annular digital twin.

and equilibrium mapping vary with fluid formulation and gas composition. The digital twin treats these as uncertain parameters within a bounded set and uses passivity-based estimation to prevent unstable drift when closures are imperfect.

The next step is to construct a storage function that captures the energy stored in compressibility and gravity, together with an internal storage associated with dissolved inventory. The port-Hamiltonian structure then expresses the system as an interconnection of energy-storing and dissipative components with boundary ports. This is developed in the next section.

3 Port-Hamiltonian Structure with Bounded Thermodynamic Exchange

The port-Hamiltonian framework represents a dynamical system in terms of an energy function and a power-conserving interconnection structure, augmented by dissipation [14]. In hydraulics, the core energy terms are compressibility-related storage and gravitational potential. In a dissolution-aware setting, additional internal energy-like terms can be introduced to represent the thermodynamic tendency of dissolved gas toward equilibrium. The goal here is not to reproduce full chemical thermodynamics, but to construct a bounded exchange mechanism that respects conservation and yields a dissipative inequality consistent with relaxation toward equilibrium.

Consider a semi-continuous state representation $x(t)$ that aggregates the distributed variables after discretization, but for clarity it is useful to begin conceptually with a distributed Hamiltonian density $\mathcal{H}(z)$ integrated over the annulus. The total stored energy is

$$H(t) = \int_0^L \mathcal{H}(z,t)\,dz \tag{1}$$

with $\mathcal{H}$ including compressibility storage, kinetic energy, and potential energy. A suitable compressibility storage for a mixture can be expressed as an integral of pressure with respect to specific volume, but in practical reduced models it is often approximated as a quadratic storage around an operating point, capturing the dominant small-signal energetics of pressure variations. Gravity contributes $\rho_m g h(z)$ terms, and kinetic energy contributes $\frac{1}{2}\rho_m u^2$.

Dissolution introduces an internal variable whose evolution is driven by an equilibrium map [15]. To represent this in an energy framework, one can define a convex potential $\Phi(x_d; p, T)$ whose minimizer with respect to x_d is the equilibrium dissolved fraction $x_d^\star(p,T)$. The relaxation exchange can then be written as a gradient flow with respect to Φ, producing dissipation in Φ while conserving total gas mass. This construction yields a Lyapunov-like term that decreases under relaxation. Because the digital twin does not seek to compute chemical free energy precisely, Φ is treated as a surrogate convex function whose derivative yields a bounded restoring force toward equilibrium. The key is that the exchange term should not inject energy; it should dissipate the mismatch between x_d and $x_d^\star$.

Component	Nominal relation	Main uncertain parameters	Operational effect
Equilibrium dissolved fraction	$x_d^\star(p,T)$	Solubility strength, composition proxies	Sets partition between dissolved and free gas at depth
Swelling factor	$B_l(x_d,p,T)$	Swelling coefficients, bounding parameters	Modifies liquid density and volumetric returns to pits
Gas density closure	$\rho_g(p,T,Z)$	Compressibility factor, effective molar mass	Influences pressure waves and gas expansion energetics
Mixture viscosity	$\mu_m(\rho_m,u)$	Friction multipliers, rheology parameters	Controls dissipation rate and pressure-drop response
Dissolution kinetics	κ_d	Interfacial area and rate scalings	Limits how fast dissolved and free inventories re-partition

Table 2: Thermodynamic and rheological closures that govern dissolution, swelling, and dissipation behavior.

Location / signal	Variables	Description	Use in architecture
Pump inlet	$q_{\rm in}$, $p_{\rm sp}$	Inflow rate and standpipe pressure	Input port defining injected hydraulic power
Choke outlet	$q_{\rm out}$, p_c	Outflow rate and choke pressure	Output port where boundary power is measured
Casing head	$p_{\rm cas}$	Surface casing pressure	Additional port for structural limits and diagnosis
Pit system	$\Delta V_{\rm pit}$	Integrated pit-volume change	Primary volumetric indicator affected by swelling
Control commands	Choke and pump setpoints	Actuation signals defining time-varying boundary conditions	Known inputs to digital twin and observers

Table 3: Boundary ports and surface measurements used by the passivity-constrained digital twin.

A generic port-Hamiltonian form for a finite-dimensional discretization is

$$\dot{x} = \big(J(x) - R(x)\big)\,\nabla H(x) \quad + \quad G(x)\,u \quad + \quad d \tag{2}$$

where J is skew-symmetric and encodes power-conserving interconnection, R is positive semidefinite and encodes dissipation, Gu encodes boundary ports and inputs, and d represents bounded disturbances such as influx [16]. The energy balance follows from

$$\begin{aligned}\dot{H} &= \nabla H^\top \dot{x} \\ &= -\nabla H^\top R \nabla H \quad + \quad \nabla H^\top G u \quad + \quad \nabla H^\top d\end{aligned} \tag{3}$$

because $\nabla H^\top J \nabla H = 0$ by skew symmetry. The dissipation term is nonpositive, and the input term represents supplied power through ports.

In an annular hydraulics discretization, the port variables correspond to boundary pressures and flows. A common representation is to choose the input u as boundary flow commands or boundary pressure commands, with G mapping these to the state derivatives. The supply rate $u^\top y$ emerges naturally as the boundary power, with y a conjugate output. In managed pressure drilling, a choke setpoint and pump rate are the effective inputs, and the conjugate outputs are boundary pressures and flows [17]. Because choke behavior is itself dissipative, it can be modeled either as part of the plant or as part of the environment, but in either case the port representation should preserve power consistency.

Frictional dissipation is encoded in R through terms proportional to flow and viscosity, typically nonlinear and state dependent. The exact friction law is uncertain, but passivity analysis does not require its exact form; it requires only that friction dissipates energy, which can be enforced by bounding the friction law within a set of

Uncertainty category	Representative examples	Treatment in model
Friction and rheology	Friction factors, cuttings-loading multipliers	Bounded parameters entering dissipation matrix R
Thermodynamic exchange	Solubility strength, swelling coefficients, κ_d	Bounded maps and rates in internal storage and exchange
Gas property correlations	Density and viscosity correlation error	Interval scaling on closures affecting H and R
Sensor bias and noise	Pit-level offset, pressure bias, lag	Explicit bias states with bounded adaptation
Influx and losses	Kick rate, onset, location, losses to formation	Disturbance inputs d_k bounded in energy balance
Model truncation	Reduced-order hydraulics and network layout	Residual term w_k in discrete energy inequality

Table 4: Main uncertainty and disturbance channels represented in the passivity-based digital twin.

Component	Symbol / structure	Interpretation	Modeling notes
Hamiltonian	$H(x)$	Stored energy in compressibility, gravity, and internal inventories	Chosen convex in key variables to define error energy
Interconnection	$J(x) = -J^\top(x)$	Power-conserving coupling of storage elements	Encodes flow/pressure network topology
Dissipation	$R(x) \succeq 0$	Friction and thermodynamic relaxation losses	Includes bounded friction and dissolution dissipation
Input map	$G(x)$	How boundary ports inject or extract power	Connects pump and choke ports to internal states
Disturbance input	d	Influx and unmodeled effects	Enters energy balance as additional power source

Table 5: Key elements of the port-Hamiltonian representation of dissolution-aware annular hydraulics.

monotone dissipative maps. This is important because friction is a dominant uncertainty source, and the digital twin should remain stable even when the nominal friction correlation is wrong. The passivity framework allows friction uncertainty to be represented as an uncertainty in the dissipation rate rather than as an uncertainty that can destabilize the system.

Dissolution exchange is incorporated by augmenting H with the convex mismatch potential Φ and by including an internal dissipative term in R that drives the dissolved fraction toward equilibrium [18]. The exchange is constructed to conserve total gas mass. In a discrete setting, this can be achieved by defining an exchange operator that transfers mass between free and dissolved inventories without changing their sum. The gradient of Φ provides the driving force, and the exchange rate is bounded. The result is that the internal thermodynamic relaxation contributes a nonnegative dissipation term in the energy balance, reflecting that mismatch to equilibrium decays.

The port-Hamiltonian form also provides a convenient way to represent influx as a disturbance entering through a port. An influx introduces gas mass and potentially energy. If influx is treated as a disturbance d, then $\nabla H^\top d$ captures the rate of energy injection associated with influx [19]. In early diagnosis, the magnitude of this term is uncertain, but the energy framework still provides a bound: if the observed boundary power and dissipation cannot account for the inferred energy growth, then an unmodeled source such as influx is implicated. This observation becomes relevant in the certification layer, where energy residuals are used to detect inconsistencies.

The thermodynamics-aware modeling of swelling affects the Hamiltonian through density and compressibility.

Aspect	Discretization choice	Intended benefit
Spatial representation	Lumped-volume or finite-volume network along the annulus	Preserves conservative coupling and power-conjugate ports
Interconnection update	Incidence-based discrete J structure	Maintains power conservation in the semi-discrete model
Time stepping	Semi-implicit scheme for storage and flows	Ensures a discrete energy inequality with numerical damping
Dissolution update	Local implicit relaxation conserving gas mass	Guarantees decrease of mismatch potential without stiffness issues
Positivity and bounds	Transformed variables for densities and fractions	Enforces physical invariants without non-physical projection
Uncertainty envelope	Bounded residual w_k in energy balance	Captures closure and truncation error for certification layer

Table 6: Structure-preserving discretization features used to retain passivity and physical admissibility.

Element	Description	Primary purpose	Addresses
State observer	Passivity-based update using output injection	Stabilize estimation under strong actuation	Pressure and flow state reconstruction
Parameter adaptation	Passive update of friction and exchange parameters	Compensate closure errors within bounds	Friction and thermodynamic mismatch
Bias estimation	Slow adaptation of sensor bias states	Separate instrumentation drift from physical change	Pit and pressure offsets
Unknown-input residual	Energy-consistent disturbance channel	Capture effects not explained by modeled ports	Influx and loss signatures
Error-energy storage	Bregman divergence induced by H	Provide quantitative bound on estimation error	Certificate consistency and robustness

Table 7: Main components of the passivity-based estimation strategy for the digital twin.

Swelling modifies liquid density and thus gravitational potential. It also modifies the mapping between mass flow and volumetric flow at surface, which affects boundary power. By embedding swelling within the constitutive relations used to compute H and the port variables, the digital twin ensures that swelling-driven volumetric changes influence the energy balance consistently [20]. This consistency is essential for interpretability; otherwise, the digital twin might attribute swelling-induced pit gain to spurious energy injection.

A critical practical requirement is boundedness and positivity of states. Phase fractions and densities must remain physical. In a port-Hamiltonian discretization, hard clipping of states can break energy consistency and break passivity. Instead, bounded coordinate transforms and invariant-region-preserving updates are used, so that the state remains physical while the energy balance remains valid. The next section develops a structure-preserving discretization strategy that maintains passivity under time stepping and under implicit thermodynamic exchange.

4 Structure-Preserving Discretization and Positivity without Projection

The port-Hamiltonian structure is valuable only if it is preserved, at least approximately, in the discrete-time digital twin used online [21]. Many numerical schemes that are stable in a forward simulation sense do not preserve passivity, especially when nonlinear dissipation and stiff source terms are present. Moreover, common enforcement mechanisms for positivity, such as clipping negative densities, introduce non-physical energy injection or removal and create non-differentiable behavior that can destabilize estimation. The discretization strategy in this paper

Quantity	Construction	Interpretation / use
Bottomhole-pressure bound	Map H and error energy to $\lvert p_{\text{bh}} - p_{\text{ref}} \rvert$ via storage norms	Certifies maximum deviation from target window over short horizons
Surface gas-handling proxy	Map gas inventories and exchange bounds to potential free-gas outflow	Provides conservative bound on near-term gas-rate loading
Pit excursion bound	Combine swelling-modified volume and density with inventory bounds	Limits plausible pit-volume change attributable to hydraulics
Energy residual	Difference between boundary power, dissipation, and storage change	Diagnostic for unmodeled energy sources such as influx or severe bias
Regime indicator	Comparison of swelling-consistent and free-gas-consistent explanations	Aids discrimination between dissolution-buffered and free-gas-dominated behavior

Table 8: Certificate-level outputs derived from the digital twin energy balance and estimation-error bounds.

therefore prioritizes discrete-time passivity and invariant-region preservation.

Spatial discretization can be constructed using a finite-volume representation where each cell stores conservative quantities and exchanges flux with neighbors. For a hydraulics network interpretation, the annulus can also be represented as a chain of lumped volumes connected by resistive elements, which naturally yields a port-Hamiltonian structure when pressure storage is associated with each volume and flow is associated with each connection. This network view is particularly suitable for managed pressure operation because it emphasizes boundary power flow and dissipation along the conduit. The state variables then include cell pressures and connection flows, along with cell gas inventories [22].

In a discrete port-Hamiltonian network, the interconnection matrix J corresponds to a signed incidence structure that couples pressure storage to flow and enforces power conservation in the absence of dissipation. Dissipation enters through resistive elements whose constitutive relations map flow to pressure drop. If these constitutive relations are monotone and dissipative, then discrete passivity follows. This representation avoids the need to resolve sharp spatial gradients that may not be identifiable from surface measurements and instead focuses on the energetics of integrated segments.

Time discretization must also preserve passivity. A backward Euler step applied to a passive system yields a passive discrete update under mild conditions because it introduces numerical damping [23]. However, backward Euler can be overly dissipative and can bias the energy residual used for certification. A midpoint or trapezoidal rule can preserve energy more accurately for conservative interconnection but may require careful treatment of dissipation to avoid numerical energy creation. The present approach uses an implicit-explicit split: interconnection and compressibility storage are advanced with a semi-implicit rule that preserves a discrete energy inequality, while stiff dissolution exchange is advanced implicitly in a way that guarantees decrease of the mismatch potential Φ.

A convenient discrete-time energy inequality can be expressed as

$$H_{k+1} - H_k \leq \Delta t\, u_k^\top y_k \quad - \quad \Delta t\, \mathcal{D}_k \quad + \quad \Delta t\, w_k \tag{4}$$

where $\mathcal{D}_k \geq 0$ is the computed dissipation and w_k is a bounded modeling residual capturing discretization error and closure uncertainty. The digital twin computes $\mathcal{D}_k$ from friction and dissolution exchange, and it estimates an envelope for w_k from uncertainty bounds. This inequality is the basis for certification. The discretization is designed so that $\mathcal{D}_k$ is not polluted by non-physical clipping or by numerical oscillations.

Positivity and boundedness are preserved by representing densities and fractions in transformed coordinates. For example, densities can be represented in logarithmic form so that positivity is automatic, and dissolved fraction can be represented by a sigmoid transform [24]. However, port-Hamiltonian structure often prefers conservative variables. The present approach therefore maintains conservative inventories for gas mass and uses transforms only for the internal reconstruction of fraction and density used in constitutive relations. The conservative update remains physically meaningful, and the reconstruction is designed to be smooth and bounded.

Dissolution exchange is treated as a local implicit update that conserves total gas mass in each cell. The update transfers mass between free and dissolved inventories according to a bounded relaxation toward equilibrium. The equilibrium map is evaluated from a thermodynamic proxy or table. The implicit update is constructed so that the mismatch potential decreases [25]. This can be achieved by choosing a convex Φ and performing a backward Euler step on the gradient flow. Because the update is local, its computational cost is small, and it can be executed at each time step even in real time.

Scenario	Main features	Dominant ambiguity	Key observation
Nominal MPD operation	Time-varying choke and pump with no influx	Separating control-induced transients from true anomalies	Observer remains stable; certificates indicate low risk
Swelling-buffered influx	Small kick at high pressure with strong dissolution	Relating pit gain to hidden dissolved inventory vs free gas	Certificates highlight pit and density risk with modest surface-gas bound
Free-gas-dominated influx	Weak dissolution or slow kinetics with migrating gas	Timing and magnitude of surface gas-rate escalation	Surface-gas proxy bound increases; uncertainty widens due to slip effects
Friction change event	Increased friction from cuttings loading	Distinguishing dissipative change from energy injection	Energy residual remains small; friction adaptation explains pressure rise
Sensor bias drift	Slowly varying pit-level or pressure offset	Misinterpreting bias as influx or loss	Bias states absorb drift; residual flags instrumentation issues when bounds exceeded

Table 9: Representative numerical study scenarios used to assess stability, ambiguity resolution, and certificate behavior.

Uncertainty in thermodynamic maps and in friction is incorporated not by random perturbation during discretization but by bounding the dissipation and exchange rates. This is important because the certification layer relies on conservative bounds. If uncertainty were treated as random noise in the discrete update, the energy inequality would not yield a deterministic certificate. Instead, the digital twin maintains interval bounds for uncertain parameters and propagates their effect into a bound on w_k [26]. The next section will show how these bounds enter observer design and certificate computation.

The discretization strategy yields a stable forward digital twin, but the central operational use is estimation under partial measurements. Estimation must not break the passivity structure. Many observer designs inject output errors into states in a way that can create energy and destabilize the system. Passivity-based observers avoid this by using output injection that is itself passive with respect to an error storage. The next section derives such observers for dissolution-aware states and uncertain parameters.

5 Passivity-Based State and Parameter Estimation under Sparse Measurements

State estimation for annular hydraulics is difficult because surface measurements provide only indirect access to internal distributions, and because unknown influx and uncertain closures can produce similar surface signatures [27]. A passivity-based estimator does not claim to identify every internal field uniquely. Instead, it aims to produce a stable estimate that remains consistent with measured boundary power and that provides conservative bounds on hidden inventories. The passivity structure yields an estimation-error energy that cannot grow unboundedly if the injection is designed appropriately, even under time-varying inputs.

Let the discrete-time digital twin be written as $x_{k+1} = f(x_k, u_k; \theta) + d_k$, where θ collects uncertain parameters and d_k represents disturbances such as influx. Let measurements be $y_k = h(x_k, u_k) + b_k + \nu_k$, where b_k is sensor bias and ν_k is noise. The estimator maintains an estimate $\hat{x}_k$ and possibly an estimate $\hat{\theta}_k$ and $\hat{b}_k$. The goal is to design an update that uses measurement residuals to correct the estimate without injecting non-physical energy.

A passivity-based observer can be constructed by adding an output injection term that is the gradient of a convex function of the output error, mapped through the adjoint of the output map. In a port-Hamiltonian setting, a natural injection uses co-energy variables and collocation at the ports [28]. Conceptually, if the plant is passive from input u to output y, then an observer error system can be made passive by injecting the difference between measured and estimated outputs through a passive feedback. This yields an inequality of the form

$$\mathcal{E}_{k+1} - \mathcal{E}_k \leq -\Delta t \, \lambda \, \|e_k\|^2 \quad + \quad \Delta t \, \eta_k \tag{5}$$

where $\mathcal{E}_k$ is an error energy, e_k is an output error, $\lambda > 0$ is a gain-like constant, and η_k collects bounded disturbance terms. The inequality implies boundedness and, when disturbances are small, convergence.

To construct such an observer, one defines an error storage as a Bregman divergence induced by the Hamiltonian, comparing the true state and the estimated state. In practice, the true state is not known, but one can analyze the estimator by assuming a true trajectory exists. The Bregman divergence is [29]

$$\mathcal{E}(x, \hat{x}) = H(x) - H(\hat{x}) - \nabla H(\hat{x})^\top (x - \hat{x}) \tag{6}$$

which is nonnegative when H is convex in the relevant variables. While the full hydraulics Hamiltonian may not be globally convex, local convexity around operating regimes can be enforced by choosing storage in terms of pressure deviations and inventories, which are convex. The observer is then designed to decrease $\mathcal{E}$ along trajectories.

In addition to state estimation, parameter adaptation is needed because friction and thermodynamic exchange rates vary. A passivity-friendly adaptation law treats parameter error as an additional energy storage and drives it down using regressor signals derived from measurable quantities. The adaptation must be bounded and projected onto plausible ranges to prevent drift. The passivity structure helps identify which parameter directions can be adapted safely from available measurements and which should remain bounded nuisance parameters.

Thermodynamic exchange parameters, such as dissolution kinetics and swelling coefficients, influence the mapping between pit-volume change and pressure signals [30]. If pit bias is present, these parameters can be confounded. The observer therefore includes an explicit bias state for pit measurements, modeled as slowly varying. The bias state is updated with a small gain and constrained by bounds. This prevents the estimator from forcing dissolution parameters to explain what is more plausibly bias drift. The observer also treats influx as an unknown input disturbance. Rather than estimate influx directly as a deterministic quantity, the observer estimates a residual power or residual mass imbalance that must be explained by disturbances. This residual becomes a diagnostic quantity: if it persists and cannot be explained by bounded model mismatch, then an influx hypothesis becomes more likely [31].

A key operational objective is to distinguish swelling-driven pit gain from free-gas-driven pit gain. In the estimator, swelling is associated with changes in dissolved inventory and liquid density, while free-gas-driven pit gain is associated with changes in free-gas inventory and compressibility. The passivity-based observer uses pressure measurements to constrain density and hydrostatics, and it uses flow measurements to constrain volumetric balance. When pressure rises under choke actuation and pit gain continues, a swelling-consistent explanation becomes more plausible because increased pressure tends to increase solubility and can increase swelling, whereas free gas would tend to compress and reduce volume. The estimator does not hard-code this logic; it emerges from the coupled model and from the measurement update, but stability is ensured by passivity constraints that prevent aggressive injection that would fit noise.

Thermodynamic modeling of swelling provides a mechanistic basis for the state representation and parameter bounds [32]. Manikonda et al. (2021) advanced an early thermodynamic swelling model for drilling mud under kick conditions, using phase-behavior concepts to quantify volumetric expansion attributable to dissolved gas and thereby clarifying how swelling can persist even when free gas is limited [33]. In the present framework, such insights inform the selection of bounded parameter ranges for swelling response and the design of the dissolved inventory state, while the observer design remains centered on passivity and error-energy decay rather than on any single thermodynamic correlation.

The result of estimation is not only $\hat{x}_k$ but also an error-energy bound. Because the observer is designed to be dissipative, one can compute an upper bound on the estimation error energy given bounds on disturbances and noise. This bound is useful for safety certification: a certificate based on a state estimate is meaningful only if the estimate error is bounded. The passivity-based estimator provides such a bound in a natural way. The next section uses these bounds, together with the plant energy inequality, to compute conservative safety indicators for bottomhole pressure and surface risk proxies.

6 Energy-Balance Certificates for Safety Monitoring and Regime Interpretation

A digital twin is operationally valuable when it produces actionable quantities that remain reliable under uncertainty [34]. Point estimates of hidden states can be misleading if the uncertainty is large or if the estimator is biased. Energy-balance certificates provide a complementary output: a bound on what the system can do given the observed boundary power, estimated dissipation, and bounded uncertainties. In a managed pressure context, such certificates can be used to bound bottomhole pressure deviation and to bound the rate at which a free-gas hazard could develop at surface, while accounting for the possibility that pit gain is driven by swelling.

The starting point is the discrete energy inequality for the plant. Over a horizon of N steps, summing the inequality yields

$$H_{k+N} - H_k \le \sum_{j=k}^{k+N-1} \Delta t\, u_j^\top y_j \quad - \quad \sum_{j=k}^{k+N-1} \Delta t\, \mathcal{D}_j \quad + \quad \sum_{j=k}^{k+N-1} \Delta t\, w_j \tag{7}$$

The boundary power term is computed from measured or commanded pressures and flows, with sign conventions [35]. The dissipation term is computed from the digital twin using estimated states and parameter bounds, producing an interval for $\sum \mathcal{D}_j$. The residual term w_j captures modeling error and unmodeled disturbances. Bounds on w_j are constructed from closure uncertainty bounds and from estimator error-energy bounds.

From this inequality, one can bound H_{k+N}. To relate energy to safety variables, one uses inequalities that map H to bounds on pressure deviation and inventories. For example, if pressure storage is represented as a quadratic term around an operating point, then H upper bounds $\|p - p_0\|^2$ in an energy norm. This yields a bound on bottomhole pressure deviation. Similarly, if the Hamiltonian includes a convex term in gas inventory and if the mapping from inventory to surface gas handling has monotone bounds, then one can bound surface gas rate proxies. The certificates are conservative because they rely on inequalities rather than on exact prediction, but they remain valid under bounded uncertainties [36].

The certificate layer must also handle the distinction between swelling-buffered and free-gas-dominated hazards. Swelling affects pit volume and density but does not necessarily imply near-term surface gas handling. The certificate therefore computes separate bounds for pit excursion and for free-gas surface rate. It uses the estimated dissolved inventory and its bound to determine how much gas could be present as free gas under worst-case exsolution within the horizon. Because dissolution exchange is bounded by kinetics and by equilibrium maps, one can bound the rate at which dissolved gas could become free gas under depressurization. This provides a conservative upper bound on how rapidly surface free gas could increase if pressure decreases. Conversely, if pressure increases, the bound can indicate that free gas is less likely to grow rapidly, but pit swelling might increase [37]. These directional conclusions are important for decisioning under managed pressure actuation.

The certificate layer also provides an interpretive diagnostic: an energy residual. If the measured boundary power minus computed dissipation implies a net energy growth that is inconsistent with the digital twin given bounded uncertainties, then an unmodeled energy source is implicated. In the annular context, such a source could be an influx that introduces gas mass and expands, or it could be a sensor bias that misreports boundary power. The certificate therefore combines the energy residual with bias bounds to decide whether the residual is more plausibly physical or instrumental. This diagnostic is complementary to statistical change detection because it relies on an energy balance rather than on pattern similarity [38].

Because property uncertainty influences dissipation and storage, certificate tightness depends on the uncertainty representation. Gas viscosity and density correlations influence friction and hydrostatics, and correlation error can persist even after calibration. Representing such uncertainty explicitly is essential for conservative certificates. The certificate design therefore incorporates parameter bounds that reflect plausible correlation deviations, motivated by empirical correlation error levels in relevant regimes [13]. This does not require the certificate to know the true correlation error; it requires a conservative envelope that prevents underestimation of risk.

The certificate layer is designed to be fast. It uses the digital twin estimate and precomputed norm equivalences between energy and pressure deviation. It uses simple monotone bounds for mapping inventories to surface gas proxies [39]. It uses interval arithmetic for uncertainty propagation. This allows the certificate to update at the same cadence as measurements and control actions. The result is a pair of outputs: a real-time estimate of state and inventories, and a real-time bound on what could happen under worst-case within the uncertainty set.

To assess how these outputs behave in practice, the next section reports numerical studies. The emphasis is not on achieving perfect prediction but on demonstrating stability under actuation, interpretability under swelling ambiguity, and conservative behavior of certificates under closure mismatch.

7 Numerical Studies and Comparative Behavior under Actuation and Swelling Ambiguity

The numerical studies evaluate the proposed passivity-constrained digital twin in scenarios designed to stress the aspects that motivate the approach: aggressive boundary actuation, ambiguity between swelling and free gas, and uncertainty in closures and sensor bias. The studies use a simplified annular configuration with representative lengths and diameters and with managed pressure boundary control signals [40]. A truth model is used to generate measurement streams. The truth model includes compressibility, friction, and dissolution exchange with swelling, and it uses parameter settings that differ from the digital twin within bounded uncertainty envelopes. This ensures that the digital twin is evaluated in a realistic mismatch regime rather than in a self-consistent simulation.

The first scenario is nominal managed pressure operation without influx. Pump rate and choke setpoint are varied to maintain bottomhole pressure near a target while responding to routine transients. In this scenario, the digital twin should remain stable and should not infer spurious gas inventory growth [41]. The passivity-based observer maintains bounded estimation error, and the energy residual remains within the uncertainty envelope. When sensor noise is introduced, the observer does not amplify it into unphysical oscillations because output injection is dissipative. The certificate layer reports small bounds on bottomhole pressure deviation consistent with measured port power and dissipation. This scenario demonstrates that the method does not generate false alarms purely due to actuation, which is a necessary condition for practical deployment.

The second scenario introduces a swelling-buffered early influx at depth. The influx rate is small and occurs under high pressure so that dissolution is significant. Pit volume begins to rise due to swelling-modified volumetric returns, but surface gas fraction remains low [42]. Choke actuation continues, producing pressure transients that overlap with influx effects. In this scenario, a free-gas-only interpretation can overpredict near-term surface gas handling risk. The digital twin estimates increased dissolved inventory with bounded free-gas inventory, and the certificate layer reports elevated pit excursion risk while keeping the surface free-gas proxy bound moderate over short horizons when pressure is maintained or increased. When pressure is decreased, the certificate bound on free-gas growth increases due to potential exsolution, reflecting a physically consistent directional risk shift. The key observation is that the method produces differentiated risk outputs under the same pit trend, aligning with the idea that pit gain is not uniquely a free-gas signal.

The third scenario introduces a free-gas-dominated influx with weaker dissolution or slower kinetics. Free gas accumulates and migrates, producing stronger compressibility signatures in pressure and flow relationships [43]. The digital twin estimates increased free-gas inventory and reports a higher bound on surface gas proxy within the horizon. The certificate layer becomes more conservative because the energy associated with free-gas expansion is larger and because slip uncertainty makes timing uncertain. The observer remains stable, but uncertainty bounds widen, reflecting that early free-gas evolution is more sensitive to slip and friction uncertainty than swelling-buffered behavior is. This widening is desirable because it prevents false precision.

The fourth scenario introduces a friction change without influx, such as increased cuttings loading. This scenario tests whether the digital twin misattributes friction-induced pressure changes to influx [44]. The passivity structure treats friction as dissipation; an increase in friction increases dissipation for a given flow. If pressure rises due to increased friction, the digital twin can explain this without introducing an energy source. The energy residual therefore remains small. The observer's parameter adaptation can adjust friction within bounds without destabilizing. Pit changes remain small, and the dissolved inventory estimate does not drift significantly. This demonstrates that the energy balance helps separate dissipative changes from energy-injecting disturbances.

The fifth scenario combines sensor bias drift with actuation [45]. Pit-volume drift is introduced as a slowly varying bias. A detector that relies on pit gain might infer influx. In the present method, pit bias is estimated as a separate state with bounds, and the passivity observer prevents bias from forcing large state deviations because injection is limited by error-energy decay. The certificate layer interprets energy residuals in light of bias bounds; if boundary power calculations depend on biased signals, the residual can be attributed to bias within the envelope. When bias exceeds the envelope, the certificate flags inconsistency, suggesting instrumentation issues. This behavior supports operational decisioning by separating physical risk from measurement integrity risk.

Across scenarios, computational feasibility is assessed qualitatively by noting that the digital twin is low order and the certificate computations are algebraic [46]. The structure-preserving discretization avoids the need for fine spatial resolution. Dissolution exchange is local and implicit, keeping stiffness manageable. The observer update involves evaluating output residuals and applying bounded gains. These operations are compatible with real-time constraints at typical surface sensor cadences.

A recurring observation in the studies is that passivity constraints reduce the sensitivity of estimation to aggressive choke maneuvers. When choke setpoints change rapidly, pressure transients can cause standard observers to overreact and to inject large corrections that destabilize internal states, especially near phase appearance [47]. In the passivity observer, the injection is dissipative relative to the error energy, preventing such instability. This stabilizing effect improves interpretability, because the estimated dissolved and free-gas inventories vary smoothly and reflect consistent energy accounting rather than numerical artifacts.

The studies also illustrate a limitation: certificates can be conservative when uncertainty envelopes are large, particularly for surface gas proxy bounds that depend on slip uncertainty. In such cases, the certificate correctly reflects limited information rather than producing spurious confidence. Tightening the envelope requires additional measurements or improved calibration. The passivity framework supports calibration by allowing parameter adaptation while preserving stability, but identifiability remains constrained by sensor availability and excitation. The present paper focuses on stability and certification rather than on optimal experiment design, but the architecture is compatible with adding excitation strategies if operationally acceptable [48].

Overall, the numerical studies indicate that a passivity-constrained digital twin can provide stable estimation and conservative risk indicators in scenarios where dissolution and swelling create ambiguity. The method is not presented as a replacement for detailed simulation or for well-control procedures. It is presented as a robust real-time layer that maintains physical consistency under uncertainty and provides interpretable outputs grounded in energy accounting.

8 Conclusion

This paper presented a passivity-constrained digital-twin architecture for managed pressure drilling in regimes where gas dissolution and mud swelling can buffer free gas and obscure early kick signatures. The approach formulated a dissolution-aware annular model with explicit partitioning between free and dissolved gas inventories and swelling-modified constitutive relations, then cast the resulting dynamics into a port-Hamiltonian structure that yields a provable energy balance with dissipation under friction and bounded thermodynamic exchange. Structure-preserving discretization strategies were described to maintain discrete-time passivity and positivity without non-physical projection, and passivity-based observers were developed to ensure estimation-error energy decay under sparse measurements, sensor bias, and time-varying boundary actuation. An energy-balance certificate layer mapped the digital twin's storage and dissipation accounting into conservative online bounds on bottomhole-pressure deviation and surface risk proxies, enabling decision thresholds that remain meaningful under bounded closure uncertainty [49].

References

[1] V. Simonov, "Problems of deep drilling in abnormally pressured zones of the kara sea continental shelf," in *Offshore Technology Conference*, OTC, May 6, 1996. DOI: 10.4043/8154-ms

[2] H. R. Briscoe, "Stabilized foamed acid, a new stimulation technique for carbonate gas reservoirs," in *SPE Permian Basin Oil and Gas Recovery Conference*, SPE, Feb. 22, 1979. DOI: 10.2118/8141-ms

[3] K. Manikonda, A. R. Hasan, O. Kaldirim, N. Rahmani, and M. A. Rahman, "Estimating swelling in oil-based mud due to gas kick dissolution," in *International conference on offshore mechanics and arctic engineering*, American Society of Mechanical Engineers, vol. 84430, 2020, V011T11A039.

[4] J. Elward-Berry and E. Thomas, "Rheologically stable deepwater drilling fluid development and application," *IADC/SPE Drilling Conference*, Feb. 15, 1994. DOI: 10.2118/27453-ms

[5] A. Mahmood, L. Ring, A. Alajbegovic, and S. Nienhuis, "Enabling new techniques: Nitrogen gas qualification and testing of a rotating control device," in *IADC/SPE Managed Pressure Drilling & Underbalanced Operations Conference & Exhibition*, SPE, Mar. 28, 2017. DOI: 10.2118/185290-ms

[6] N. Kanaujia, J. Singh, and A. S. Kalamdhad, "Biogas development in india: A sustainable energy for future," in Springer International Publishing, Jun. 24, 2021, pp. 145–155. DOI: 10.1007/978-3-030-70463-6_14

[7] N. Kim, "Study of the pvt behavior of methane and ester-based drilling fluid mixtures," in *SPE Annual Technical Conference and Exhibition*, SPE, Sep. 19, 2010. DOI: 10.2118/141130-stu

[8] G. M. Matilla, *Diseño de los sistemas de comunicación en plantas de exploración y producción de hidrocarburos*, Sep. 27, 2013.

[9] N. Adams, "Well control. part 9. supplemental rig equipment has vital job," *Oil & Gas Journal*, vol. 78, Jan. 21, 1980.

[10] L. Hoberock and S. Stanbery, "Pressure dynamics in wells during gas kicks: Part 2 - component models and results," *Journal of Petroleum Technology*, vol. 33, no. 08, pp. 1367–1378, Aug. 1, 1981. DOI: 10.2118/9822-pa

[11] T. Nagashima et al., "High-quality ion beam generation in laser plasma interaction," in *Proceedings of the 12th Asia Pacific Physics Conference (APPC12)*, vol. 2, Journal of the Physical Society of Japan, Mar. 19, 2014, pp. 015 093–. DOI: 10.7566/jpscp.1.015093

[12] J. Ursin, "Fault block modelling-an alternative simulation tool for strongly compartmentalized gas reservoirs," *Journal of Canadian Petroleum Technology*, vol. 40, no. 11, Nov. 1, 2001. DOI: 10.2118/01-11-02

[13] A. K. Sleiti et al., "Comprehensive assessment and evaluation of correlations for gas-oil ratio, oil formation volume factor, gas viscosity, and gas density utilized in gas kick detection," *Journal of Petroleum Science and Engineering*, vol. 207, p. 109 135, 2021.

[14] J. Feng, J. Fu, P. Chen, and L. Xu, "Investigation of methane/drilling mud phase behavior and its influence to hydrocarbon drilling activity," *Energy Science & Engineering*, vol. 7, no. 4, pp. 1280–1291, Apr. 21, 2019. DOI: 10.1002/ese3.345

[15] A. S. Prakoso, *Penanggulangan well kick pada sumur "adr 01" lapangan "talang jimar " blok south sumatera dengan metode engineerpt. pertamina utc*, Aug. 1, 2015.

[16] M. Tingay, "Initial pore pressures under the lusi mud volcano, indonesia," *Interpretation*, vol. 3, no. 1, SE33–SE49, Dec. 15, 2014. DOI: 10.1190/int-2014-0092.1

[17] E. Messana, "Data acquisition and recording system," in *Offshore Technology Conference*, OTC, Apr. 30, 1979. DOI: 10.4043/3418-ms

[18] X. Sun, B. Sun, Y. Gao, and Z. Wang, "A model of multiphase flow dynamics considering the hydrated bubble behaviors and its application to deepwater kick simulation," *Journal of Energy Resources Technology*, vol. 140, no. 8, pp. 082 004–, May 29, 2018. DOI: 10.1115/1.4040190

[19] N. B. Cook, *Failure evidence for all 21 ipcc positive-feedback climate models*, Feb. 1, 2013.

[20] J. Billingham, M. Thompson, and D. White, "Advanced influx analysis gives more information following a kick," *SPE/IADC Drilling Conference*, Feb. 22, 1993. DOI: 10.2118/25710-ms

[21] M. Suezawa, "Hydrogen-point defect complexes in electron-irradiated c-doped and high-purity si," *Japanese Journal of Applied Physics*, vol. 38, no. 6, pp. 608–610, Jun. 1, 1999. DOI: 10.1143/jjap.38.l608

[22] B. DeJarnett, L. Krystinik, R. Mead, and S. Poe, *Greater green river basin production improvement project, phase 1: Site characterization report*, May 1, 1996. DOI: 10.2172/578487

[23] B. W. Atchison, "Automated well control: From automated detection to automated shut-in," in *SPE/IADC Middle East Drilling Technology Conference and Exhibition*, SPE, May 25, 2021. DOI: 10.2118/202091-ms

[24] B. McKernan et al., "Ram-pressure stripping of a kicked hill sphere: Prompt electromagnetic emission from the merger of stellar mass black holes in an agn accretion disk," *The Astrophysical Journal Letters*, vol. 884, no. 2, pp. L50–, Oct. 17, 2019. DOI: 10.3847/2041-8213/ab4886

[25] L. A. G. de Faria, P. Ribeiro, N. A. Policarpo, N. R. Kim, and A. T. P. Falcade, "Use of correlations for pvt characteristics of drilling fluids in kick analysis," *Revista dos Trabalhos de Iniciação Científica da UNICAMP*, no. 26, Feb. 11, 2019. DOI: 10.20396/revpibic262018849

[26] J. M. Gundlach, "Section 115 in practice," in Edward Elgar Publishing, Oct. 15, 2020. DOI: 10.4337/9781786434616.00009

[27] S. Q. Tunio, A. H. Tunio, N. A. Ghirano, and S. Irawan, *Is it possible to ignore problems rising during vertical drilling? a review*, Nov. 25, 2011.

[28] J. Zhang, J.-M. Richter, and C. Kaczmarek, "Catalysts for post euro 6 plug-in hybrid electric vehicles," *SAE International Journal of Advances and Current Practices in Mobility*, vol. 2, no. 6, pp. 3151–3163, Apr. 14, 2020. DOI: 10.4271/2020-01-0354

[29] D. Lagerlef, W. Smalstig, and M. Erwin, "Gas-lift-valve test rack opening design methodology for extreme kickoff temperature conditions," in *SPE Western Regional Meeting*, SPE, Mar. 30, 1992. DOI: 10.2118/24065-ms

[30] K. S. Bjorkevoll, J. O. Skogestad, J. Frøyen, and H. Linga, "Well control simulator: Enhancing models with compositional pvt models and kinetics," in *IADC/SPE Drilling Conference and Exhibition*, SPE, Mar. 6, 2018. DOI: 10.2118/189651-ms

[31] R. J. Lunn, *Options for scotland's gas future*, Jun. 30, 2015.

[32] P. Qin, A. Andreanov, H. C. Park, and S. Flach, *Interacting ultracold atomic kicked rotors: Loss of dynamical localization*, Mar. 1, 2017.

[33] K. Manikonda et al., "A gas kick model that uses the thermodynamic approach to account for gas solubility in synthetic-based mud," in *SPE/IADC Middle East drilling Technology conference and exhibition*, SPE, 2021, D031S016R001.

[34] B. Patel, T. D. Cooper, and W. Billings, "The application of advanced gas extraction and analysis system complements early kick detection & control capabilities of managed pressure drilling system with added hse value," *SPE/IADC Drilling Conference*, Mar. 5, 2013. DOI: 10.2118/163498-ms

[35] D. Gomes, J. Frøyen, K. K. Fjelde, and K. S. Bjorkevoll, "A numerical comparison and uncertainty analysis of two transient models for kick management in a backpressure mpd system," in *SPE Norway One Day Seminar*, SPE, Apr. 18, 2018. DOI: 10.2118/191345-ms

[36] T. Bourgeois, "Auger tension leg platform: Conquering the deepwater gulf of mexico," in *International Petroleum Conference and Exhibition of Mexico*, SPE, Oct. 10, 1994. DOI: 10.2118/28680-ms

[37] J. Bang, S. Mjaaland, L. K. Jensen, and P. Hendriks, *Brief : Acoustic gas-kick detection with wellhead sonar*, Feb. 1, 1995.

[38] J. Sharma, T. Cuny, O. Ogunsanwo, and O. L. A. Santos, "Low-frequency distributed acoustic sensing for early gas detection in a wellbore," *IEEE Sensors Journal*, vol. 21, no. 5, pp. 6158–6169, Mar. 1, 2021. DOI: 10.1109/jsen.2020.3038738

[39] S. M. M. Sarshar, "The applications of a novel compact separation system in ubd and mpd operations," in *IADC/SPE Managed Pressure Drilling and Underbalanced Operations Conference and Exhibition*, SPE, Apr. 17, 2013. DOI: 10.2118/164570-ms

[40] D. Gomes, J. Frøyen, K. K. Fjelde, and K. S. Bjorkevoll, "Transient modelling and sensitivity analysis of influxes in backpressure mpd systems," in *SPE Asia Pacific Oil and Gas Conference and Exhibition*, SPE, Oct. 23, 2018. DOI: 10.2118/192101-ms

[41] A. T. Beck, D. L. Cecílio, W. J. de Santana Gomes, R. K. Tessari, and C. M. C. Jacinto, "Empirical random kick model and casing reliability," *SPE Drilling & Completion*, vol. 35, no. 04, pp. 644–654, May 22, 2020. DOI: 10.2118/201200-pa

[42] D. Foreman, "Earth first! 3, no. 3," *Eearth*, vol. 3, Mar. 21, 1983.

[43] D. Strickland and M. Smith, *Concentric workovers successful in a well recovery operation*, Jun. 1, 1997.

[44] C. Jie, M. Sun, and Z. Li, "Research on the formation pressure prediction in the exploration area of northeast sichuan, china," in *International Oil and Gas Conference and Exhibition in China*, SPE, Jun. 8, 2010. DOI: 10.2118/131396-ms

[45] X. Sun, J. B. Qu, T. Yan, and L. Wang, "Numerical simulation for gas-liquid two-phase flow along the borehole after air cutting," *Advanced Materials Research*, vol. 821-822, pp. 1414–1417, Sep. 18, 2013. DOI: 10.4028/www.scientific.net/amr.821-822.1414

[46] K. Bybee, "Drilling underbalanced from a drillship in the santos basin," *Journal of Petroleum Technology*, vol. 58, no. 04, pp. 74–76, Apr. 1, 2006. DOI: 10.2118/0406-0074-jpt

[47] P. Liu, H. Yin, T. X. Wang, and M. Han, "Analysis of the pressure response of kick control in mpd," *Advanced Materials Research*, vol. 997, pp. 713–716, Aug. 11, 2014. DOI: 10.4028/www.scientific.net/amr.997.713

[48] M. Volonteri, *Evolution of massive black holes*, Sep. 12, 2007.

[49] J. Schubert, H. C. Juvkam-Wold, J. Choe, and D. T. Dreher, "Analysis of gas kicks in multilateral wells utilizing computer simulation," *IADC/SPE Drilling Conference*, Feb. 21, 2006. DOI: 10.2118/99028-ms